V International Conference on Computational Methods for Coupled Problems in Science and Engineering
COUPLED PROBLEMS 2013
S. Idelsohn, M. Papadrakakis and B. Schrefler (Eds)

DEVELOPMENT OF A MAXIMUM ENTROPY APPROACH FOR THE THERMOMECANICAL MODELLING OF THE ROTARY FRICTION WELDING PROCESS

M. FOCA*, G. RACINEUX† AND L. STAINIER†

*Institut de Recherche en Gnie Civil et Mcanique (GeM, UMR 6183 CNRS)
Ecole Centrale de Nantes
44300 Nantes, France
e-mail: mathieu.foca@ec-nantes.fr

†Institut de Recherche en Gnie Civil et Mcanique (GeM, UMR 6183 CNRS)
Ecole Centrale de Nantes
44300 Nantes, France
e-mail: guillaume.racineux@ec-nantes.fr & laurent.stainier@ec-nantes.fr

Key words: Thermo-dynamical coupling, Maximum Entropy, Meshfree, Rotative Frictional Welding

Abstract. A multi-physics modelling of rotary friction welding process based on a Maximum Entropy approach is proposed. This approach will be able to solve coupled thermo-mechanical problems. Because strains are very high locally around the welded area, the remeshing time in a classical finite element method is very important. The use of this meshless method should reduce simulations time and the numerical diffusion phenomena.

1 INTRODUCTION

The Rotary Friction Welding (RFW) is used to assemble two parts one of which at least has a symmetry of revolution. It uses the thermical effects created by the friction between the rotating part and the fixed one. The heating power is resulting of resisting torque and rotation speed. The melting temperature is not reached because of the material creep during the welding and forging. One of the advantages of the RFW compared to other welding process such as resistance welding or laser beam welding is that the welded area has an exceptional quality. Nowadays, two kinds of rotary friction welding are mainly used: direct drive and inertial welding.

2 MODELLING

In order to obtain a good numerical modelling of the process, all thermical and mechanical aspects have to be taken care of. Therefore, the thermo-mechanical coupling

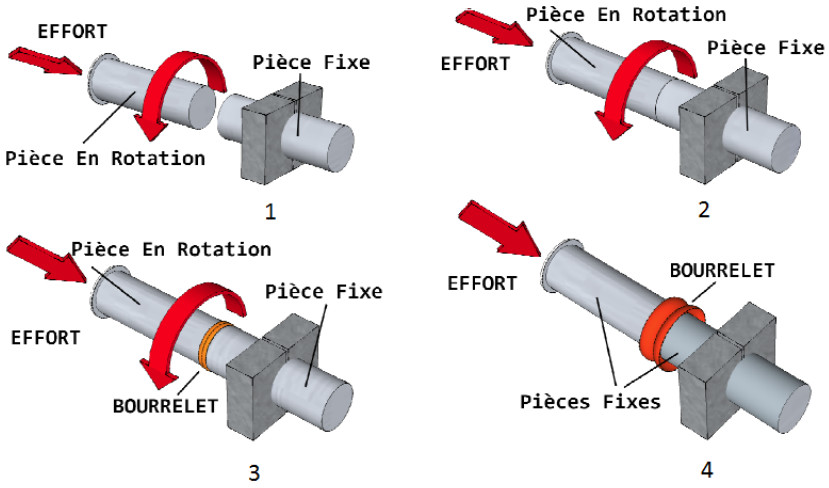

Figure 1: Rotary friction welding principle.

happening during the welding cannot be ignored. Indeed, there are very high strains and temperatures can reach high values near the welded area. So having a calculation code able to take care of all these parameters is very important. The whole study will be performed in axisymmetric 2D because of the symmetry of revolution of the moving part. To evaluate the efficiency of our method, the results we obtain will be compared to the results of an equivalent simulation performed on Abaqus, which will be considered as the industrial reference. For such a simulation, Abaqus remeshes the structured as soon as the upset is reaching a certain value: for example, it does not simulate more than 0.5mm with a same mesh. Then we obtain a mesh evolution showed on figure 2. The two main drawbacks of the use of finite element method is that remeshing takes a lot of time and results in propagation of numerical errors. This last aspect is really important in our context because an objective is to perform metallurgy analysis after the welding and it requires a very precise temperature field during the simulation.
The maximum entropy method has been prefered to other meshless method such as Smoothed Particuled Hydrodynamics (SPH) or Element Free Galerkin because we have to deal with contacts and therefore to exactly define the edges.
The long-term objective is to be able to solve general thermo-mechanical problems. Bibliographic references [1] [2] shows that the method gives good results on mechanical problem with an adiabatic behaviour.

3 EXPERIMENTAL ASPECT

Experiments are lead in partnership with ACB on a RDS60 machine in order to compare the results we obtain by simulation. In a first time, P295GH steel parts are melt. It can be thick or thin tubes or solid cylinder. Once the influence of each parameter is set, titanium alloy TA6V will be weld.

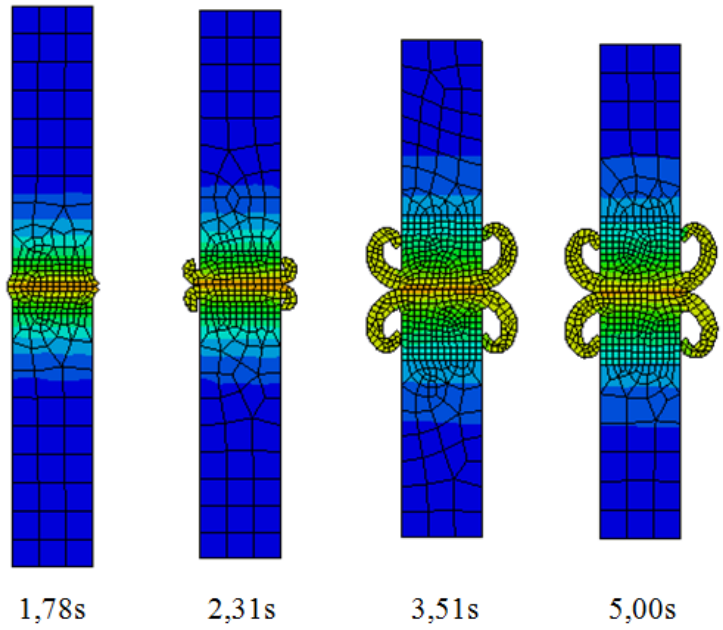

Figure 2: Mesh evolution using Abaqus [3]

The RFW process is made of four stages:

- Phase 1 : Force increasing.
- Phase 2 : Friction phase at constant force and rotation speed.
- Phase 3 : Force increasing until the imposed forge force.
- Phase 4 : Cooling under constant force.

The following parameters are set on the machine. Indicated values correspond to our first experimental test plan.

- Force applied to the moving part: between 35kN and 155kN.
- Rotation speed V : between 600 tr/min and 900 tr/min.
- Material consuming U: material quantity ejected during the welding, between 4mm and 8mm.

The objective is to compare the following aspects:

- Heating time.

- Material consuming speed.
- Temperature field.
- Influence of the forge force.
- Size of the Thermical Affected Area (TAA).

Moreover, the use of a thermal camera gives us the temperature field on the part surface around the welded area.

4 MAXIMUM ENTROPY METHOD

4.1 Origins

The MaxEnt method uses the entropy defined by Shannon [4] in the information theory. In this theory, entropy is defined as a measure of uncertainty. To find a solution maximizing the entropy means that we want to find the most uncertain solution. Here is an example. Let's take a set of event A = $\{A_1, ..., A_n\}$ linked to the probabilities $\{p_1, ..., p_n\}$. Let's consider the two following cases:

$$B_1 = \begin{pmatrix} A_1 & A_2 \\ 0.5 & 0.5 \end{pmatrix} \text{ and } B_2 = \begin{pmatrix} A_1 & A_2 \\ 0.9 & 0.1 \end{pmatrix}$$

The most uncertain result is obviously obtained in the case B_1. Therefore the entropy is higher in case B_1 than B_2. Based on three criteria, Shannon [4] established the entropy H expression as following:

$$H(B) = H(p_1, ..., p_n) = -\sum_{a=1}^{n} p_a \log p_a \tag{1}$$

We obtain:

$$H(B_1) = 0.301 \text{ et } H(B_2) = 0.141$$

4.2 Linear Maximum Entropy problem

Consider a set of distinct nodes $X = \{\mathbf{x}_a, a = 1, ..., N\} \subset \mathbb{R}^d$. The smallest convex space containing X is define as following [5]:

$$convX = \{\mathbf{x} \in \mathbb{R}^d | \mathbf{x} = \mathbf{X}\boldsymbol{\lambda}, \boldsymbol{\lambda} \in \mathbb{R}^N_+, \mathbf{1}.\boldsymbol{\lambda} = 1\} \tag{2}$$

where $\mathbb{R}^N_+$ is the positive orthant, $\mathbf{1} \in \mathbb{R}^N$ is the vector full of 1 and $\mathbf{X}$ is a d x N matrix in which columns represent the coordinates of nodes in X. As X is finite, $convX$ is convex and compact.

Let $u : convX \to \mathbb{R}$ whom values $\{u_a = u(x_a), a = 1, ..., N\}$ are known on X. We want to build approximations of u (which may represent a displacement field for example) having the following form:

$$u^h(\mathbf{x}) = \sum_{a=1}^{n} p_a(\mathbf{x}) u_a \tag{3}$$

where functions $p_a : convX \to \mathbb{R}$ are the *shape functions*. Those functions must respect the following conditions:

$$\sum_{a=1}^{n} p_a(\mathbf{x}) = 1 \tag{4}$$

$$\sum_{a=1}^{n} p_a(\mathbf{x}) \mathbf{x}_a = \mathbf{x} \tag{5}$$

Arroyo and Ortiz [1] proved that it is possible to make a link between those relationship and Shannon's entropy. In order to respect Jaynes [6] maximum entropy principle, the following problem (ME) must be solved:

$$\begin{array}{lll} \text{(ME)} & \text{Maximise} & H(\mathbf{p}) = -\sum_{a=1}^{n} p_a \log p_a \\ & & \\ & \text{such as} & p_a \geqslant 0, a = 1, ..., N \\ & & \sum_{a=1,}^{n} p_a(\mathbf{x}) = 1 \\ & & \sum_{a=1,}^{n} p_a(\mathbf{x}) \mathbf{x}_a = \mathbf{x} \end{array}$$

Moreover, in order to control the correlation degree between the shape functions values in x and values at close nodes, a locality notion has to be add. Then the following (RAJ) problem [7] must be solved:

$$\begin{array}{lll} \text{(RAJ)} & \text{For } \mathbf{x} \text{ fixed, minimise} & U(\mathbf{x}, \mathbf{p}) \equiv \sum_{a=1}^{n} p_a |\mathbf{x} - \mathbf{x_a}|^2 \\ & & \\ & \text{such as} & p_a \geqslant 0,\ a = 1, ..., N \\ & & \sum_{a=1}^{n} p_a(\mathbf{x}) = 1 \\ & & \sum_{a=1}^{n} p_a(\mathbf{x}) \mathbf{x}_a = \mathbf{x} \end{array}$$

To obtain the best compromise between the two aspects, the following problem must be solved:

$$\begin{array}{lll} \text{(LME)}_\beta & \text{For } \mathbf{x} \text{ fixed, minimise} & f_\beta(\mathbf{x}, \mathbf{p}) \equiv \beta U(\mathbf{x}, \mathbf{p}) - H(\mathbf{p}) \\ & & \\ & \text{such as} & p_a \geqslant 0,\ a = 1, ..., N \\ & & \sum_{a=1}^{n} p_a(\mathbf{x}) = 1 \\ & & \sum_{a=1}^{n} p_a(\mathbf{x}) \mathbf{x}_a = \mathbf{x} \end{array}$$

Arroyo et Ortiz [1] also proved that the solution to the $(\text{LME})_\beta$ problem is unique and has the following expression:

$$p_{\beta a} = \frac{1}{Z(\mathbf{x}, \boldsymbol{\lambda}^*(\mathbf{x}))} \exp[-\beta|\mathbf{x} - \mathbf{x}_a|^2 + \boldsymbol{\lambda}^*.(\mathbf{x} - \mathbf{x}_a)] \tag{6}$$

where:

$$Z(\mathbf{x}, \boldsymbol{\lambda}) = \sum_{a=1,}^{n} \exp[-\beta|\mathbf{x} - \mathbf{x}_a|^2 + \boldsymbol{\lambda}.(\mathbf{x} - \mathbf{x}_a)] \tag{7}$$

$$\boldsymbol{\lambda}^*(\mathbf{x}) = \arg \min_{\boldsymbol{\lambda} \in \mathbb{R}^d} \log Z(\mathbf{x}, \boldsymbol{\lambda}) \tag{8}$$

$\boldsymbol{\lambda}$ correspond to Lagrange multipliers imposing (4) and (5) conditions.
β must be set during the simulation depending on the interpolation degree we want to. $\beta = 0$ means that the shape function support is $convX$ whereas $\beta = +\infty$ means that the entropy aspect is neglected. For all $\beta \in [0, +\infty[$ and for all $\mathbf{x} \in \text{conv}X$, the solution exists and is unique. The parameter γ, linked to β as following, is generally used:

$$\gamma = h^2\beta \tag{9}$$

where h the characteristic length between two nodes.

5 FIRST RESULTS

In references, MaxEnt method has only be used to solve mechanical problem [1] [2]. Before solving coupled thermo-mechanical problems, we check that we have good results on simple thermical cases. Matlab code shared by Arroyo and Ortiz is used as base.

5.1 Shape functions visualisation

5.1.1 Shape functions in 1D

In this 1D example, we have five nodes at following coordinates:

$$x_a = 0.01a, \quad \forall a \in [0; 1; 2; 3; 4]$$

Here, $h = 0.01$. The figure 3 represents the five shape functions for different value of γ. Values in table 5.1.1 prove that conditions (4) and (5) are satisfied.

5.1.2 Shape functions in 2D

In the same way, shape functions in 2D are presented on figure 4.

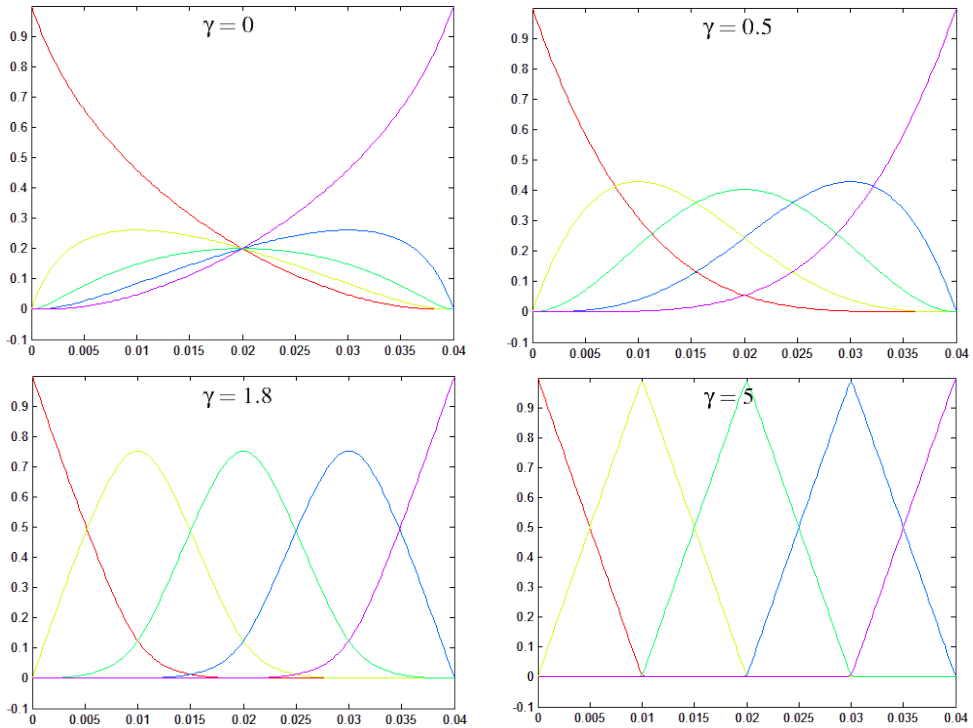

Figure 3: Shape functions in 1D for different values of γ, $\gamma = \{0, 0.5, 1.8, 5\}$.

	Node 1	Node 2	Node 3	Node 4	Node 5
Function 1	1.000	$1.247e^{-1}$	$5.605e^{-4}$	$6.828e^{-8}$	$1.562e^{-27}$
Function 2	$4.401e^{-5}$	$7.511e^{-1}$	$1.241e^{-1}$	$5.558e^{-4}$	$1.740e^{-18}$
Function 3	$5.249e^{-11}$	$1.236e^{-1}$	$7.507e^{-1}$	$1.236e^{-1}$	$5.294e^{-11}$
Function 4	$1.740e^{-18}$	$5.558e^{-4}$	$1.241e^{-1}$	$7.511e^{-1}$	$4.401e^{-5}$
Function 5	$1.562e^{-27}$	$6.828e^{-8}$	$5.605e^{-4}$	$1.247e^{-1}$	1.000

Table 1: Shape functions values on a 1D example, $\gamma = 1.8$.

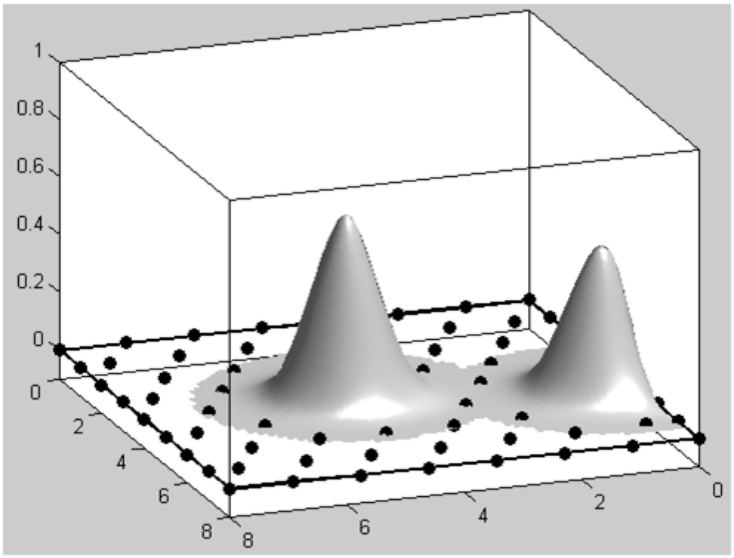

Figure 4: Fonctions de formes sur un modle 2D

5.2 Resolution of a thermical problem

The following system must be solved in order to solve a thermical problem:

$$[C]\{\dot{T}\} + [K]\{T\} = \{q_e\} \tag{10}$$

with T the vector of nodal temperatures, C the matrix of heat capacity, K the matrix of conductibility and q_e the vector of imposed flux.

5.2.1 Calculation of conductibility matrix K

The calculation of the matrix K is given by :

$$\forall(a,b), K_{a,b} = \sum_{a=1}^{n} k\boldsymbol{\nabla p_{\beta a}}.\boldsymbol{\nabla p_{\beta b}} dV \tag{11}$$

with k is the heat conductivity of the material, $\boldsymbol{\nabla p_{\beta i}}$ is the gradient of the shape function at node i, obtained by derivation of the shape function $p_{\beta i}$.

5.2.2 Calculation of the heat capacity matrix C

The calculation of the matrix C is given by :

$$\forall(a,b), C_{ab} = \sum_{a=1}^{n} \rho c_v p_{\beta a} p_{\beta b} dV \tag{12}$$

with ρ is the density of the material, c_v is the specific heat of the material, $p_{\beta i}$ is the value of the shape function at node i.
In order to compare with Abaqus results, the same C matrix must be used. Abaqus is using a C' matrix condensed on the diagonal as following.

$$\forall (i,j) \in [\![1,n]\!]^2, C'_{ij} = \delta_{ij} \sum_{k=1}^{n} C_{ik} \tag{13}$$

5.2.3 Numerical integration

We solve the system by a temporal integration using finite differences. In particular, we use the generalized method of the trapezius:

$$\begin{cases} [C']\{\dot{T}_{n+1}\} + [K]\{T_{n+1}\} = \{q_e(t_{n+1})\} \\ \{T_{n+1}\} = \{T_n\} - (1-\alpha)\Delta t\{\dot{T}_n\} + \alpha\Delta t\{\dot{T}_{n+1}\} \end{cases} \tag{14}$$

with:

- $\alpha = 0$: explicit scheme
- $\alpha = 1/2$: Crank-Nicholson scheme
- $\alpha = 1$: Euler-implicit scheme

Then we use the Crank-Nicholson scheme.

5.3 Test 1D, comparison MaxEnt/FEM

In order to verify the validity of our model, we compare results obtained by the two methods on simple cases. Here, we only present one of the tests.

Consider a bar of an homogeneous material of length $L = 0.03m$. Finite elements mesh and MaxEnt nodes are defined on figure 5. In this example, we note $T_0 = 273K$. At first, the temperature of the bar is set to $T = T_0$ and then $\forall t \geq 0$, the temperature on one side is set to $T = 400K$: Initial conditions:

$$T(x,0) = 0, \forall x \in]0, L]$$
$$\dot{T}(x,0) = 0, \forall x \in [0, L]$$

Boundary conditions:

$$T(0,t) = T_0, \forall t \geq 0$$

The figure 6 compare FEM and MaxEnt results. Results are very similar, which proves taht MaxEnt method is valid.

Figure 5: FEM mesh (—) and MaxEnt nodes and integration points (•) for the bar example

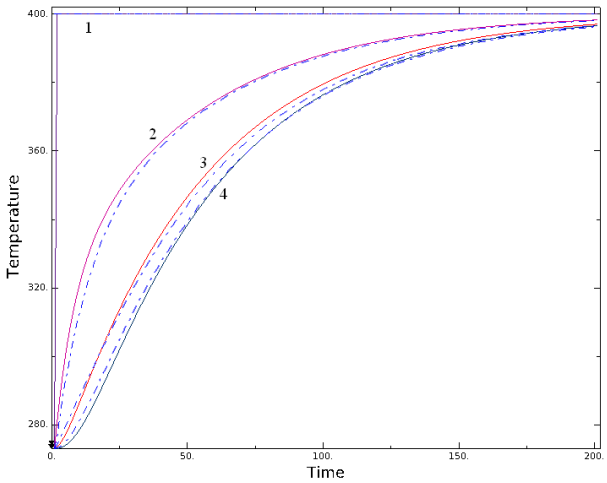

Figure 6: Comparison FEM (—) / MaxEnt (– · –) on a simple thermical problem.

6 CONCLUSION

In this work, an application of the maximum entropy principle for the resolution of coupled thermo-mechanical problems has been proposed. The consistency on mechanical problems [1][2] and on simple thermical problems encourages us to continue. After we implement the code to compute this method, we should be able to simulate the rotary friction welding process and we should have results accurate enough then to perform metallurgical studies.

Thanks

This work is a part of the Friction Rotative à Entrainement Direct (FRED) project, funded by OSEO, in collaboration with ACB, ENSAM (LAMPA) and Polytech' Nantes (IMN).

REFERENCES

[1] M. Arroyo, M. Ortiz. *Local maximum-entropy approximation schemes: a seamless bridge between finite elements and meshfree methods*, International journal for numerical methods in engineering, 65:2167-2202, 2006.

[2] B. Li, A. Kidane , G. Ravichandran, M. Ortiz. *Verification and validation of the Optimal Transportation Meshfree (OTM) simulation of terminal ballistics*, INT J IMPACT ENG, 42:25-36, 2012.

[3] Abaqus Example Problems Manual, *1.3.18 Inertia welding simulation using Abaqus/Standard and Abaqus/CAE*, SIMULIA, Abaqus 6.10.

[4] C. E. Shannon. *A Mathematical Theory of Communication*, The Bell System Technical Journal, diteur, 27:379-423, 27:623-656, 1948.

[5] R. T. Rockafellar. *Convex Analysis*, Princeton University Press, Princeton NJ, 1970.

[6] E. T. Jaynes. *Information theory and statistical mechanics*, Physical Review, **106**(4):620-630, 1957.

[7] V. T. Rajan. *Optimality of the Delaunay triangulation*, Discrete and Computational Geometry, **12**(2)189-202, 1994.